Charged Current Neutrino Cross Section and Tau Energy Loss at Ultra-High Energies

N. Armesto[1], C. Merino[2], G. Parente[3], and E. Zas[4]

Departamento de Física de Partículas &
Instituto Galego de Física de Altas Enerxías
Universidade de Santiago de Compostela
15706 Santiago de Compostela, Spain

Abstract

We evaluate both the tau lepton energy loss produced by photonuclear interactions and the neutrino charged current cross section at ultra-high energies, relevant to neutrino bounds with Earth-skimming tau neutrinos, using different theoretical and phenomenological models for nucleon and nucleus structure functions. The theoretical uncertainty is estimated by taking different extrapolations of the structure function F_2 to very low values of x, in the low and moderate Q^2 range for the tau lepton interaction and at high Q^2 for the neutrino-nucleus inelastic cross section. It is at these extremely low values of x where nuclear shadowing and parton saturation effects are unknown and could be stronger than usually considered. For tau and neutrino energies $E = 10^9$ GeV we find uncertainties of a factor 4 for the tau energy loss and of a factor 2 for the charged current neutrino-nucleus cross section.

[1]nestor@fpaxp1.usc.es
[2]merino@fpaxp1.usc.es
[3]gonzalo@fpaxp1.usc.es
[4]zas@fpaxp1.usc.es

1 Introduction

The detection of high energy neutrinos is one of the most important challenges in Astroparticle Physics. Conventional neutrino detectors exploit the long range of muons produced by muon neutrino charged current (CC) interactions [1]. With the discovery of neutrino flavor oscillations it has been realized that also tau neutrinos reach the Earth in spite of being heavily suppressed in all postulated production mechanisms. The possibility to search for tau neutrinos by looking for tau leptons that exit the Earth, Earth-skimming neutrinos, has been shown to be particularly advantageous to detect neutrinos of energies in the EeV range [2, 3]. The short lifetime of the tau lepton originated in the neutrino charged current interaction allows the tau to decay in flight while still close to the Earth surface producing an outcoming air shower in principle detectable by both fluorescence telescopes and air shower arrays [4]. This same channel yields negligible contributions for other neutrino flavors. The sensitivity to tau neutrinos through the Earth-skimming channel directly depends both on the neutrino charged current cross section and on the tau range (the energy loss) which determine the amount of matter with which the neutrino has to interact to produce an emerging tau [5, 6]. While the energy loss for muons is shared by roughly equivalent contributions from pair production, bremsstrahlung and photonuclear interactions, for tau leptons of energies above $E = 10^7$ GeV, photonuclear interactions (i.e. lepton-nucleus inelastic interactions dominated by small values of Q^2) are responsible for the largest and the most uncertain contribution [7, 8, 9].

Both the neutrino cross section and the tau photonuclear energy loss are calculated from theory using structure functions which carry the information of the nucleon and nucleus structure. In order to study the uncertainties in the calculation of Earth-skimming neutrinos the same structure functions should be consistently used for both processes due to their strong correlation in the resulting tau flux. Unfortunately this is not possible since the kinematical Q^2 (minus the squared momentum transfer) and Bjorken-x ranges that contribute to these processes are quite different, specially at EeV energies, and the available parameterizations are not entirely adequate to describe both ranges simultaneously.

The Q^2 scale that contributes to the tau energy loss, dominated by photon exchange,

is low and moderate Q^2 at very low x, where perturbative and non perturbative QCD effects are mixed. The CC neutrino cross section is produced by W-boson exchange that sets the relevant scale of Q^2 to values up to M_W^2 at low x, a region where perturbative QCD is expected to work. In both cases the relevant x range lies well outside the regions where structure functions are measured, so one has to rely on extrapolations which contain significant uncertainties.

The charged current neutrino cross section is usually calculated using parton distribution functions which are evolved according to perturbative QCD predictions. A number of alternative parameterizations exist, some of which allow extrapolation of the uncertainties in the fitted parameters as a mean to explore some of the uncertainties associated to the calculation. In the case of photonuclear processes existing predictions at high energy arise basically from two independent approaches, the Generalized Vector Dominance (GVD) model and Regge-like models.

In this article we study the tau energy loss (see also Ref. [10]) and the neutrino-nucleus cross section. Both quantities have direct implications for high energy neutrino detection, in particular for Earth-skimming tau neutrinos. Due to the large uncertainties in the existing models, the fact that none of them covers simultaneously the kinematical region relevant for both quantities, and the need of consistency in both calculations, we use and extend available models with the aim of estimating the theoretical uncertainty by considering extreme results. In this way, in the frame of the most relevant models, we cover the range of possible scenarios for the extrapolation of structure functions to the relevant x and Q^2 range. Two important effects to be taken into account in this extrapolation of the structure functions are nuclear shadowing corrections and saturation due to partonic screening. Nuclear corrections [11] are deviations from the naive picture in which the nucleus is treated as an incoherent sum of nucleons. Saturation [12] accounts for the fact that the structure functions cannot rise indefinitely as x goes to zero. Saturation effects may be included in nuclear corrections but are also present in the nucleon structure functions (although for smaller values of x and/or Q^2). In addition to existing calculations, a new computation of the tau energy loss and the neutrino-nucleon cross section based on saturation physics [13] is also presented in this work.

The result of the present analysis is an uncertainty band for both the tau-lepton

energy loss by photonuclear interactions and the CC neutrino-nucleus cross section. Understanding and minimizing the uncertainties in these two calculations must be considered an important priority for high energy neutrino astrophysics.

2 The photonuclear tau energy loss

The average energy loss per unit depth, X, of taus is conveniently represented by:

$$-\left\langle \frac{dE}{dX} \right\rangle = a(E) + b(E)E \ , \tag{1}$$

where $a(E)$ is due to ionization and $b(E)$ is the sum of fractional losses due to e^+e^- pair production, bremsstrahlung, and photonuclear interactions. The parameter $a(E)$ is nearly constant and the term $b(E)E$ dominates the energy loss above a critical energy that for tau leptons is of a few TeV. The electromagnetic contribution to the energy loss, mainly due to pair production and bremsstrahlung, is well under control, while the photonuclear interaction which dominates for tau energies exceeding $E = 10^7$ GeV is affected by relatively large uncertainties.

The contribution to $b(E)$ from photonuclear interactions is obtained by integration of the lepton-nucleus differential cross section, $d\sigma^{lA}/dy$:

$$b(E) = \frac{N_A}{A} \int dy \, y \int dQ^2 \frac{d\sigma^{lA}}{dQ^2 dy} \ , \tag{2}$$

where N_A is Avogadro's number, A the mass number, and y the fraction of energy lost by the lepton in the interaction.

For the lepton-nucleus differential cross section we consider the general expression for virtual photon exchange in terms of structure functions:

$$\frac{d\sigma^{lA}}{dQ^2 dy} = \frac{4\pi\alpha^2}{Q^4} \frac{F_2^A}{y} \left[1 - y - \frac{Q^2}{4E^2} + \left(1 - 2\frac{m_l^2}{Q^2} \right) \frac{y^2 + Q^2/E^2}{2(1+R^A)} \right] \ , \tag{3}$$

where E is the lepton energy in the lab frame, m_l the lepton mass, and α the fine structure constant. F_2^A is the structure function F_2 for a nuclear target A which is found to be different from the mere superposition of A free nucleon structure functions F_2^p [11]. R^A is the ratio of the longitudinal to transverse structure functions which gives a small contribution to the cross section [7] and is neglected for clarity of the discussion below. The variables x, y and Q^2 are related by kinematics through $Q^2 = 2MExy$, and

both F_2 and R are functions of x and Q^2. The contribution to the tau energy loss from neutral current and γ-Z interference interactions was estimated to be small [14] and is also neglected.

The limits in the double integral of Eq. (2) are well established:

$$Q^2_{min} = \frac{y^2 m_l^2}{1-y} \,, \qquad Q^2_{max} = 2m_p E y - 2m_\pi m_p - m_\pi^2 \,, \tag{4}$$

$$y_{min} = \frac{2m_\pi m_p + m_\pi^2}{2m_p E} \,, \qquad y_{max} = 1 - \frac{m_l}{E} \,, \tag{5}$$

where m_p and m_π are the proton and pion mass, respectively.

The predictions of the photonuclear interaction cross section in the GVD Model [15] (BB) and in its extension to higher energies by including a perturbative component based on the color dipole model [16] (BS), have been widely used to explore muon and tau lepton propagation in matter (see for instance [17, 8, 9] and references therein).

The calculations in which the F_2 structure function is given by a phenomenological parameterization of data based on Regge Theory appear in Refs. [7] (DRSS), [14] (BM), [18] (KLS), and [19] (PT). For the proton structure function, F_2^p, DRSS (see also Ref. [20]) uses the ALLM model [21], while BM and KLS both consider the CKMT model [22] at low Q^2 matched at high Q^2 to perturbative QCD predictions based on different parameterizations of parton distribution functions, and PT uses the proton structure function of Ref. [23]. The F_2^p structure function is shown in Figs. 1 and 2, together with the HERA data at the lowest measured x values at different Q^2.

In DRSS, BM, and KLS calculations the nuclear structure function is related to the proton structure function through $F_2^A = f^A A F_2^p$. At high energy only the low x behavior of the nuclear correction factor f^A is relevant to the calculation of $b(E)$, as we will show below (see Fig. 6). In the DRSS calculation the low x behavior of f^A freezes at the value $f^A = A^{-0.1}$ for $x < 0.0014$ (~ 0.73 for standard rock, $A = 22$), while in the BM (and KLS) calculations f^A reaches a maximal asymptotic regime $f^A = A^{-1/3}$ (~ 0.36 for $A = 22$) at much lower x (see Fig. 3). Both DRSS and BM nuclear corrections are Q^2-independent.

In addition to the existing calculations we present a new computation of the photonuclear tau energy loss using the results of Ref. [13] (ASW) which are based on the geometric scaling property [26] that all data on $\sigma^{\gamma^* p}$ and on $\sigma^{\gamma^* A}$ lie on a single universal curve in terms of the scaling variable $\tau = Q^2/Q^2_{sat}$ whose form is inspired in saturation

physics (the detailed expressions leading to the ASW F_2 structure function are given in the Appendix). The ASW F_2 structure function for the proton case is plotted in Figs. 1 and 2 (for $x < 0.01$ where this parameterization is expected to be valid). The ASW structure function F_2 contains mild nuclear corrections at low x when compared with DRSS and BM nuclear corrections (see Fig. 3). Nuclear corrections in ASW depend on Q^2.

The photonuclear contributions to $b(E)$ computed (for standard rock $A = 22$ throughout all this paper) with ALLM and with CKMT structure functions, and the same nuclear corrections [7], give very close results (see Fig. 4). Although ALLM and CKMT parameterizations share a common theoretical base, with a reggeon and a pomeron component, and they are fitted to the same data sets, ALLM systematically lies above CKMT at low x (see Fig. 2), which accounts for the difference in $b(E)$ observed in Fig. 4.

The lowest values of $b(E)$ at high energies is obtained with the ASW structure functions. Though the ASW structure function F_2 contains mild nuclear corrections at low x, saturation effects at the nucleon level are rather strong and limit the rise of $b(E)$ with energy as observed in Fig. 4. For energies below $E = 10^6$ GeV the result from the ASW structure function is higher than those from ALLM or CKMT (see Fig. 4). This is because at low Q^2 the ASW structure function is significantly higher for the region $10^{-6} < x < 10^{-3}$ (see Fig. 2) which is the relevant range for energies below $E = 10^6$ GeV, as it can be deduced from Fig. 6. Thus the saturation-based ASW prediction lowers the energy loss rate $b(E)$ with respect to the already existing predictions by a factor 2 at $E = 10^9$ GeV, and by a factor even larger at higher energies.

The BB/BS calculation gives the largest of the predicted energy loss rates up to energies of the order $E = 10^7$ GeV. Above this scale the PT result exceeds all other existing predictions by at least a factor 2 already at $E = 10^9$ GeV (i.e. a factor 4 with respect the ASW prediction, see Fig. 4). Thus the PT prediction can be considered as an estimate of the upper limit of the tau energy loss at UHE.

Much of the uncertainty in the tau energy loss is actually due to nuclear effects. The choice of nuclear corrections from Ref. [7], Ref. [14], or from Ref. [13] (see Fig. 3), translates into differences in the calculated value of $b(E)$ (using the ALLM structure function) by a factor rising from 1.5 to 2.5 as the tau energy increases in the range $E = 10^6$-10^9 GeV (see Fig. 5). This energy range corresponds to the region of very low

x where differences in the nuclear correction factor are large. In order to quantify how much different regions of x and Q^2 contribute to $b(E)$, the dependence of $b(E)$ on the maximum value of x and on the maximum value of Q^2 considered in the integration is shown in Figs. 6 and 7.

The differential cross section $d\sigma^{\tau A}/dy$ is also a relevant quantity for high energy neutrino detection as it enters the event rate convolutions together with the neutrino flux and the experimental acceptances. Indeed it has been shown that stochastic effects of the tau energy loss distribution have significant relevance in the prediction of emerging tau rates [20]. The energy loss spectrum $yd\sigma^{\tau A}/dy$ obtained using both ALLM and ASW structure functions are compared in Fig. 8. Clearly, the energy loss spectrum calculated with ALLM is significantly harder than the one calculated with ASW. The contributions of moderate ($Q^2 > 1$) and low Q^2 ($Q^2 < 1$) (in a rough way corresponding respectively to hard and soft interactions) are shown separately in Fig. 9 for the ALLM structure function.

3 The charged current neutrino cross section

The absolute value of the cross section naturally has a direct impact on the sensitivity of experiments because the event rate is directly proportional to it, but it also enters with opposite effect in the attenuation of the neutrino beam as a function of matter depth traversed, having much impact on the angular and energy distribution of the events. These two effects combine in the case of Earth-skimming tau neutrino interactions to play an important role for the rate calculation. In addition to the tau lepton photonuclear cross section we also study how the uncertainties in the F_2 structure function at low x affect the CC neutrino deep inelastic cross section. Since in the more realistic expectations [27] the nuclear corrections to the CC neutrino-nucleon cross section decrease at low x with increasing Q^2, becoming small at high Q^2 [28], we will neglect them in our calculations.

The CC DIS neutrino-nucleon cross section is expressed in terms of the structure function F_2 as follows:

$$\frac{d\sigma_{CC}^{\nu N}}{dQ^2 dy} = \frac{G_F^2}{4\pi}\left(\frac{M_W^2}{M_W^2+Q^2}\right)^2 \frac{F_2^{\nu N}}{y}[1+(1-y)^2]\,, \tag{6}$$

where E is the neutrino energy and y the fraction of energy lost by the neutrino in the

interaction. In this expression F_L and xF_3 contributions are neglected since F_L tends to zero as Q^2 rises and xF_3 deals basically with the valence partons which hardly contribute at the low x values relevant for the cross section.

In order to consistenly use the structure functions from charged lepton interactions (as ALLM, CKMT, and ASW models) in neutrino interactions we must relate the electromagnetic and weak structure functions. The F_2 structure function for neutrino interaction is related to the F_2 structure function for charged lepton interactions by the ratio of the weak and electromagnetic couplings through $F_2^{\nu N} = 18/5\ F_2^{lN}$ (assuming a symmetric sea), although the kinematical regions of the two processes are different (low and moderate $Q^2 \sim 0.01$-10 GeV^2 in the photonuclear case and high $Q^2 \sim M_W^2$ in the high energy CC interaction). Concerning the x range the main contribution comes from low x in both cases, though x values are lower in the photonuclear case than in the CC interaction. For the calculation of the neutrino-nucleon cross section at high energies, we then use the structure function F_2 for charged lepton interaction valid up to very low x and high Q^2, instead of following the standard approach based on parton densities.

The neutrino-nucleon cross sections from ALLM and CKMT structure functions are presented in Fig. 10. They are clearly below predictions from modern parton densities [29], since the ALLM parameterization is not consistent with high Q^2 experimental points (see Fig. 1) and CKMT is not evolved to high Q^2, so we have not used them to discuss the theoretical uncertainties in the estimation of the CC neutrino-nucleon cross section. Instead we have taken the parameterization of F_2 *à la* BCDMS obtained by the SMC Collaboration [30], which correctly represents the existing experimental data at high Q^2 (see Fig. 1) and provides a smooth connection at neutrino energies around $E = 10^7$ GeV with the parton density prediction of the CC neutrino-nucleon cross section [29] (see Fig. 10).

We have performed three different extrapolations at low x of the F_2 parameterization given in Ref. [30], one following the ASW structure function, a second one from the phenomenological parameterization fitting low x HERA data [31], and the third one which corresponds to the double logarithmic approximation (DLA) in QCD from Ref. [32] (KOPA) (ASW and KOPA structure functions are valid at low x, $x < 0.01$, i.e. at high energy).

In Fig. 11 the effect of taking the three different parameterizations of the structure function F_2 at low x on the neutrino-nucleon cross section is shown. We see that in comparison with the prediction obtained with evolved QCD parton densities of Ref. [29], both KOPA (which corresponds to the DLA of perturbative QCD) and ASW (which includes strong saturation effects) estimations are below at high energies.

On the other hand the extrapolation of the HERA based parameterization with the exponent $\lambda = 0.0481 \ln(Q^2/0.292^2)$ ($F_2 \sim x^{-\lambda}$), produces an extremely fast increase of the cross section with energy (see the upper curve in Fig. 11), since this exponent rises to values above $\lambda \sim 0.5$ when Q^2 becomes large. This raw extrapolation is in contradition with perturbative calculations and we do not consider it for uncertainty estimates as it is not physically motivated. Nevertheless it is considered here to explicitely show its discrepancy with pQCD. For the more realistic scenarios, when the rise of the exponent freezes to smaller values $\lambda < 0.4$, our prediction supports the result obtained in the detailed analysis of Ref. [29]. The curves are shown in Fig. 11 (from up to down corresponding to λ frozen to $\lambda = 0.50$, 0.40, and 0.38 respectively). When considering only physically motivated extrapolations, the theoretical uncertainty at $E = 10^9$ GeV is a factor 2.

4 Conclusions

We estimate the uncertainties coming from the extrapolations of the existing models for proton and nucleus structure functions for tau energy loss and for CC neutrino-nucleon cross section. Both calculations must be done consistently within the same model as their effect on the tau flux produced by Earth-skimming neutrinos is correlated. The theoretical uncertainty in the tau energy loss is greater than that of the neutrino-nucleon CC cross section because the Q^2 region contributing to the tau energy loss cross section is lower and so are the relevant values of Bjorken-x. In addition the structure functions conventionally used for the calculation of the tau energy loss are not suitable to be used in the high-Q^2 range which is relevant for the CC neutrino-nucleon interaction. As a result systematic effects arising in the calculation of a tau neutrino bound from Earth-skimming events due to uncertainties in the structure functions turn out to be difficult to evaluate. Several extreme models allowed by extrapolation of structure functions have been explored in

order to estimate ranges for these quantities.

Below energies in the $E = 10^7$ GeV range the highest prediction for the photonuclear contribution to tau energy loss, $b(E)$, is provided by the BB/BS calculation. Above this energy range the PT result exceeds all other considered predictions while the lowest calculation is obtained using the ASW structure functions. The difference between the two extreme predictions reaches a factor 4 at $E = 10^9$ GeV and increases as the energy rises. The BB/BS, ALLM, and CKMT calculations agree within a 30 % and go approximately parallel for all energies, which is an indication of a systematic normalization difference of the structure functions in each model. The application of much stronger nuclear shadowing (than usually considered) at low x can lower the prediction of $b(E)$ with respect to the already existing calculations by a factor up to 2 at $E = 10^9$ GeV.

In the case of the CC neutrino-nucleon cross section the importance of nuclear effects at high energies is expected to be small [28]. We have also considered saturation effects in the CC neutrino-nucleon cross section by using the structure function ASW. At $E = 10^{10}$ GeV, the CC neutrino-nucleon cross section calculated with the ASW structure function is found to be half of the pQCD calculation with parton densities, in rough agreement with the evaluation of saturation effects reported in Ref. [33], and also in Ref. [34] where different parameterizations of the dipole cross section containing saturation are employed. The calculation of the neutrino cross section with the ASW structure function has also been performed in Ref. [35]. Though the quantitative agreement of our result with this calculation is reasonably good, some discrepancy appears due to the fact that to extend the validity of ASW to the region $x > 0.01$, we have connected the ASW structure function to the parameterization of HERA data *à la* BCDMS from Ref. [30].

The effect of a rapid rise of the F_2 structure function at low x in the CC neutrino-nucleon cross section has also been studied using the x-slope $\lambda(Q^2)$ of the F_2 HERA data ($F_2 \sim x^{-\lambda}$) for all Q^2 values. We have found that the cross section rises with energy very rapidly. At $E = 10^{10}$ GeV it can become a factor 4 above the pQCD calculation with parton densities. On the other hand the logarithmic rise of the structure function F_2 at small x predicted by the DLA-pQCD results in a slower increase of the CC neutrino-nucleon cross section with energy. At $E = 10^{10}$ GeV the DLA estimation is a 20 % below the pQCD calculation with parton densities. When considering only realistic extrapolations,

the theoretical uncertainty at $E = 10^9$ GeV is a factor 2.

The obtained uncertainty for the tau energy loss is to be implemented, together with the corresponding one for the CC neutrino-nucleon cross section, both in analytical and Monte Carlo calculations of the rates of taus emerging from Earth-skimming tau neutrinos, which is currently being used to calculate high energy neutrino bounds. This task is beyond the scope of this paper.

Acknowledgements

We thank O. Blanch Bigas, M.V.T. Machado, D. Pertermann, Yu.M. Shabelski, and D.A. Timashkov for useful comments on this work. N.A. acknowledges financial support by Ministerio de Educación y Ciencia (MEC) of Spain under a Ramón y Cajal contract. This work has been supported by MEC under grants FPA2005-01963 and FPA2004-01198, by Xunta de Galicia under grant 2005 PXIC20604PN and Consellería de Educación, and by FEDER Funds.

Appendix: The ASW F_2 structure function

The form of the single universal curve where all data on $\sigma^{\gamma^* p}$ and on $\sigma^{\gamma^* A}$ lie as function of the scaling variable $\tau = Q^2/Q^2_{sat}$ is motivated by saturation and given by [13, 36]:

$$\sigma^{\gamma^* p}(x, Q^2) \equiv \Phi(\tau) = \bar{\sigma}_0 \left[\gamma_E + \Gamma\left(0, \xi\right) + \ln \xi\right] , \tag{7}$$

with γ_E the Euler constant, $\Gamma\left(0, \xi\right)$ the incomplete Γ function, and $\xi = a/\tau^b$, with $a = 1.868$ and $b = 0.746$ extracted from a fit to lepton-proton data. The saturation scale $Q^2_{\rm sat}$ is parameterized as $Q^2_{\rm sat}({\rm GeV}^2) = (\bar{x}/x_0)^{-\lambda}$ [37], where $x_0 = 3.04 \cdot 10^{-4}$, $\lambda = 0.288$, and $\bar{x} = x\left(Q^2 + 4m_f^2\right)/Q^2$ with $m_f = 0.14$ GeV. The normalization is fixed by $\bar{\sigma}_0 = 40.56\ \mu$b.

The extension to the nuclear case is done through

$$\sigma^{\gamma^* A} = \frac{\pi R_A^2}{\pi R_p^2} \sigma^{\gamma^* p}(\tau_A) \tag{8}$$

and

$$Q^2_{\rm sat,A} = Q^2_{\rm sat,p} \left(\frac{A\pi R_p^2}{\pi R_A^2}\right)^{\frac{1}{\delta}} \Rightarrow \tau_A = \tau \ \left[\frac{\pi R_A^2}{A\pi R_p^2}\right]^{\frac{1}{\delta}} , \tag{9}$$

where the nuclear radius is given by the usual parameterization $R_A = (1.12A^{1/3} - 0.86A^{-1/3})$ fm, and $\delta = 0.79 \pm 0.02$ and $\pi R_p^2 = 1.55 \pm 0.02$ fm^2 are extracted from a fit to lepton-nucleus data. The nuclear structure function F_2^A is $F_2^A(x, Q^2) = Q^2\sigma^{\gamma^* A}/(4\pi^2\alpha)$. The ASW structure function for the proton case is recovered by taking $A = 1$ in the expressions above (see Figs. 1 and 2).

The functional shape of (7) is motivated by considerations in saturation physics [13, 36]. From a pragmatic point of view, it provides a very good description of existing lepton-proton and lepton-nucleus data in the region $0.01 < \tau, \tau_A < 100$ and $x < 0.01$ which for $Q^2 = 0.01, 0.1, 1$, and 10 GeV^2 corresponds to a low x limit of $\sim 10^{-5}$, 10^{-7}, 10^{-10}, and 10^{-13}, respectively. For $\tau \to 0$ F_2 behaves like a single logarithm, so $F_2 \propto \ln 1/x$ for $x \to 0$ and $F_2/A \propto \ln A/A^{1/3}$ for $A \to \infty$. Thus this model results in very large screening corrections for asymptotic values of x and A.

References

[1] T. K. Gaisser, F. Halzen and T. Stanev, Phys. Rept. 258 (1995) 173 [Erratum-ibid. 271 (1996) 355].

[2] D. Fargion, Astrophys. J. 570 (2002) 909.

[3] X. Bertou, P. Billoir, O. Deligny, C. Lachaud, and A. Letessier-Selvon, Astropart. Phys. 17 (2002) 183.

[4] E. Zas, New J. Phys. 7 (2005) 130.

[5] O. Blanch Bigas (Pierre Auger Collaboration), Proceedings of the 30th ICRC (2007), to be published.

[6] J. Alvarez-Muñiz (Pierre Auger Collaboration), Proceedings of the 30th ICRC (2007), to be published.

[7] S.I. Dutta, M.H. Reno, I. Sarcevic, and D. Seckel, Phys. Rev. D63 (2001) 094020.

[8] E.V. Bugaev, T. Montaruli, Yu.V. Shlepin, and I. Solkalski, Astropart. Phys. 21 (2004) 491.

[9] C. Aramo *et al.*, Astropart. Phys. 23 (2005) 65.

[10] N. Armesto, C. Merino, G. Parente, and E. Zas, Proceedings of the 30th ICRC (2007), to be published.

[11] M. Arneodo, Phys. Rep. 240 (1994) 301; D. F. Geesaman, K. Saito, and A. W. Thomas, Ann. Rev. Nucl. Part. Sci. 45 (1995) 337.

[12] QCD Perspectives on Hot and Dense Matter, edited by J.-P. Blaizot and E. Iancu, Kluwer, Dordrecht, The Netherlands, 2002 (NATO Science Series, II, Mathematics, Physics, and Chemistry, Vol. 87).

[13] N. Armesto, C. Salgado, and U.A. Wiedemann, Phys. Rev. Lett. 94 (2005) 022002.

[14] A.V. Butkevich and S.P.Mikheyev, Zh. Eksp. Teor. Fiz 122 (2002) 17.

[15] L.B. Bezrukov and E.V. Bugaev, Yad. Fiz. 33 (1981) 1195.

[16] E.V. Bugaev and Yu.V. Shlepin, Phys. Rev. D67 (2003) 934027.

[17] P. Lipari and T. Stanev, Phys. Rev. D 44 (1991) 3543.

[18] K.S. Kuzmin, K.S. Lokhtin, and S.I. Sinegovsky, Int. J. Mod. Phys. A20 (2005) 6956; A.A. Kochanov, K.S. Lokhtin, and S.I. Sinegovsky, arXiv:hep-ph/0508306; K.S. Lokhtin and S.I. Sinegovsky, Russ. Phys. J. 49 (2006) 326 [Izv. Vuz. Fiz. 49 (2006) 82].

[19] D.A. Timashkov and A.A. Petrukhin, Proceedings of the 29th ICRC (2005) 9, 89-92.

[20] S.I. Dutta, Y. Huang, and M.H. Reno, Phys. Rev. D72 (2005) 013005.

[21] H. Abramowicz and A. Levy, arXiv:hep-ph/9712415.

[22] A. Capella, A. Kaidalov, C. Merino, and J. Tran Thanh Van, Phys. Lett. B337 (1994) 358; A. Kaidalov, C. Merino, and D. Pertermann, Eur. Phys. J. C20 (2001) 301.

[23] A.A. Petrukhin and D.A. Timashkov, Yad. Fiz. 67 (2004) 2241 [Phys. At. Nucl. 67 (2004) 2216].

[24] C. Adloff *et al.* (H1 Collaboration), Eur. Phys. J. C21 (2001) 33.

[25] J. Breitweg *et al.* (ZEUS Collaboration), Phys. Lett. B487 (2000) 53.

[26] A.M. Stasto, K. Golec-Biernat, and J. Kwiecinski, Phys. Rev. Lett. 86 (2001) 596.

[27] N. Armesto, J. Phys. G32 (2006) R367.

[28] J.A. Castro Pena, G. Parente, and E. Zas, Phys. Lett. B507 (2001) 231.

[29] L.A. Anchordoqui, A.M. Cooper-Sarkar, D. Hooper, and S. Sarkar, Phys. Rev. D74 (2006) 043008.

[30] B. Adeva *et al.* (Spin Muon Collaboration), Phys. Rev. D58 (1998) 112001.

[31] C. Adloff *et al.* (H1 Collaboration), Phys. Lett. B520 (2001) 183.

[32] A.V. Kotikov and G. Parente, Nucl. Phys. B549 (1999) 242.

[33] K. Kutak and J. Kwiecinski, Eur. Phys. J. C29 (2003) 521.

[34] E. M. Henley and J. Jalilian-Marian, Phys. Rev. D73 (2006) 094004.

[35] M. V. T. Machado, Phys. Rev. D71 (2005) 114009.

[36] J.L. Albacete, N. Armesto, J.G. Milhano, C.A. Salgado, and U.A. Wiedemann, Eur. Phys. J. C 43 (2005) 353.

[37] K. Golec-Biernat and M. Wüsthoff, Phys. Rev. D 59 (1999) 014017.

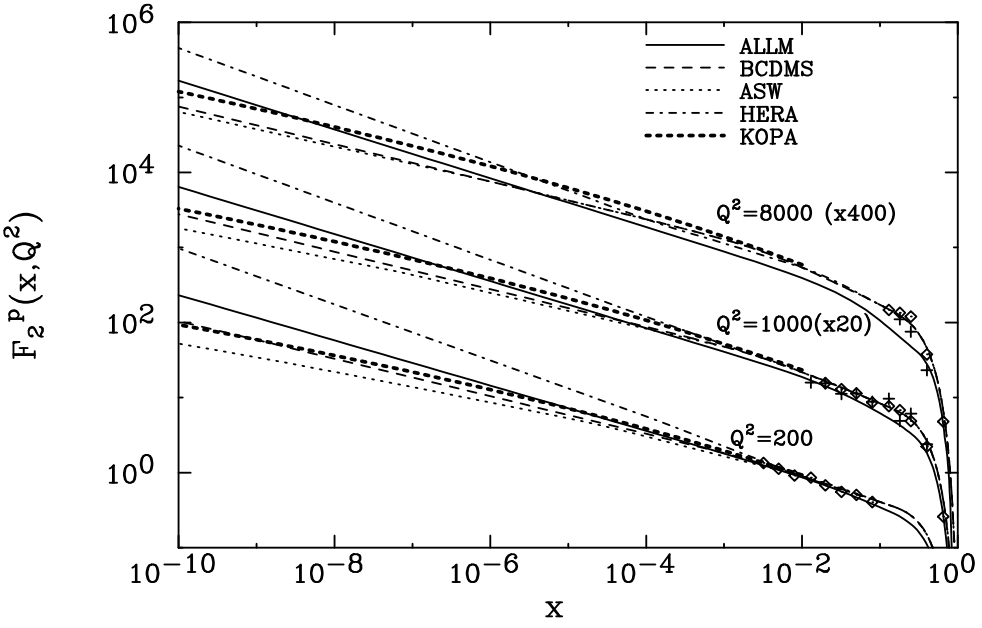

Figure 1: The proton structure function F_2 as a function of x for different high $Q^2(\mathrm{GeV}^2)$ values. Data points are from HERA [24, 25].

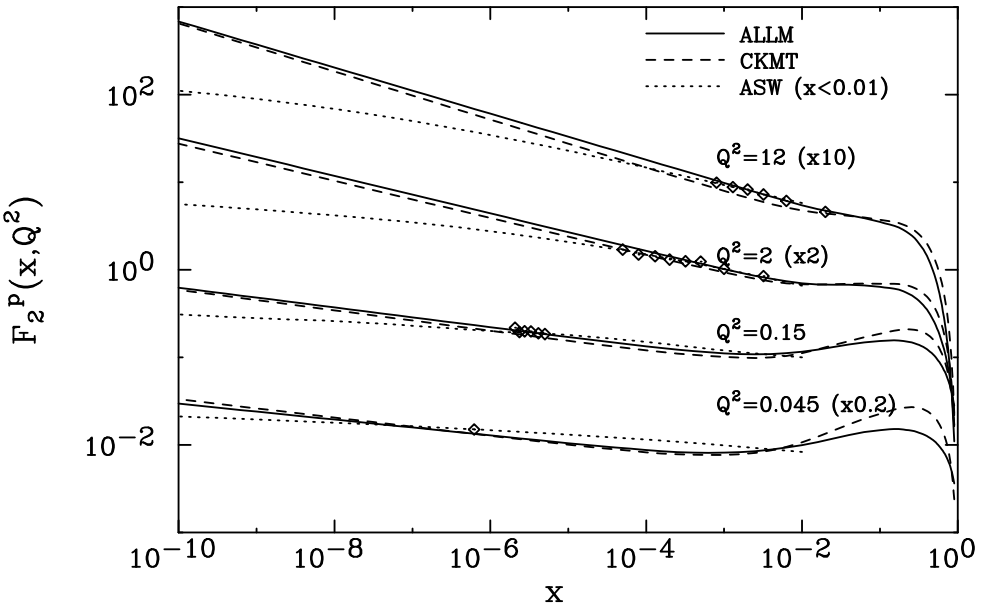

Figure 2: The proton structure function F_2 as a function of x for different low Q^2 (GeV^2) values. Data points are from HERA [24, 25].

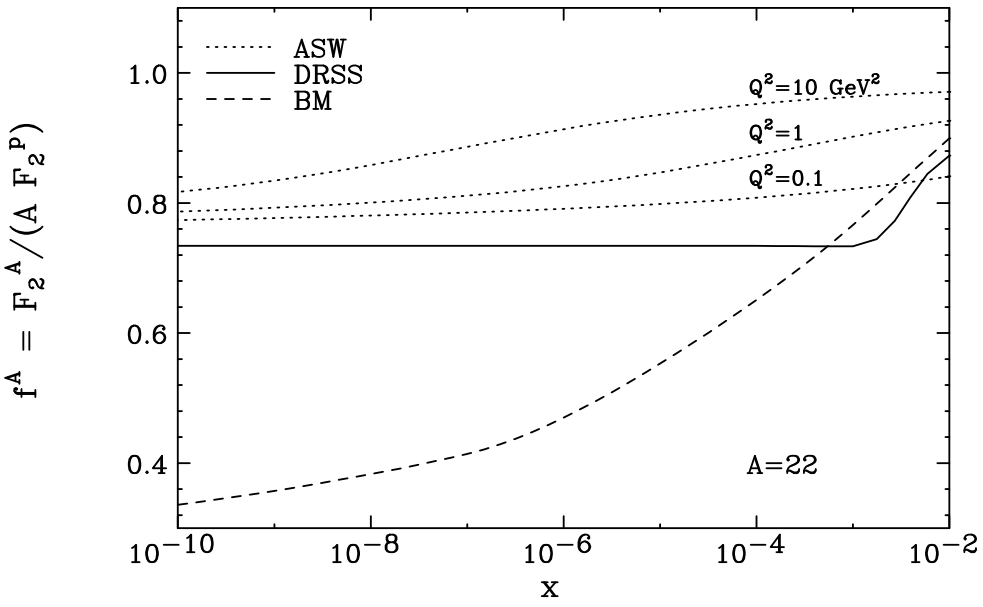

Figure 3: The nuclear correction factor f^A as a function of x.

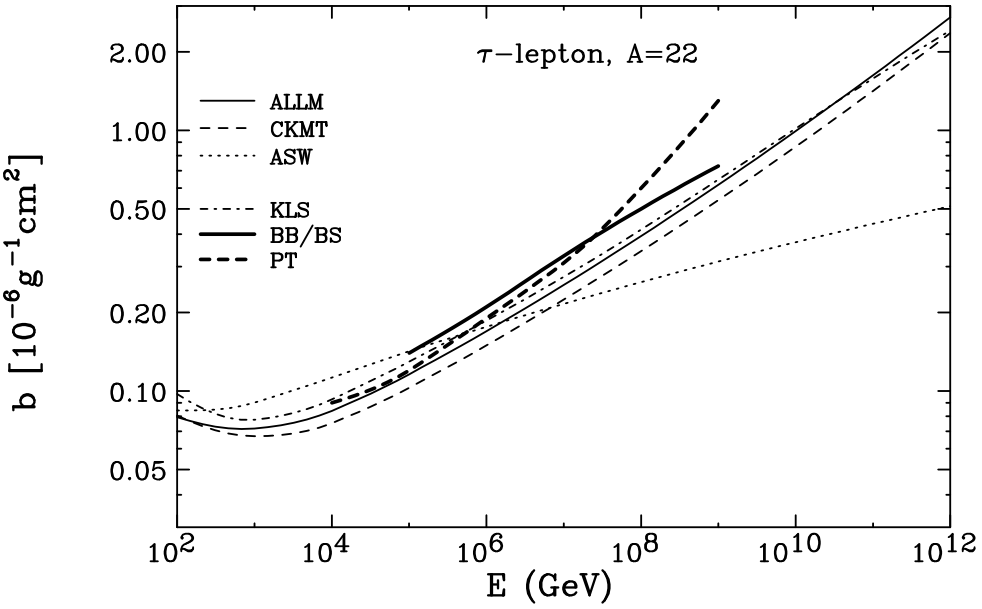

Figure 4: The photonuclear energy loss rate, $b(E)$, computed in different models.

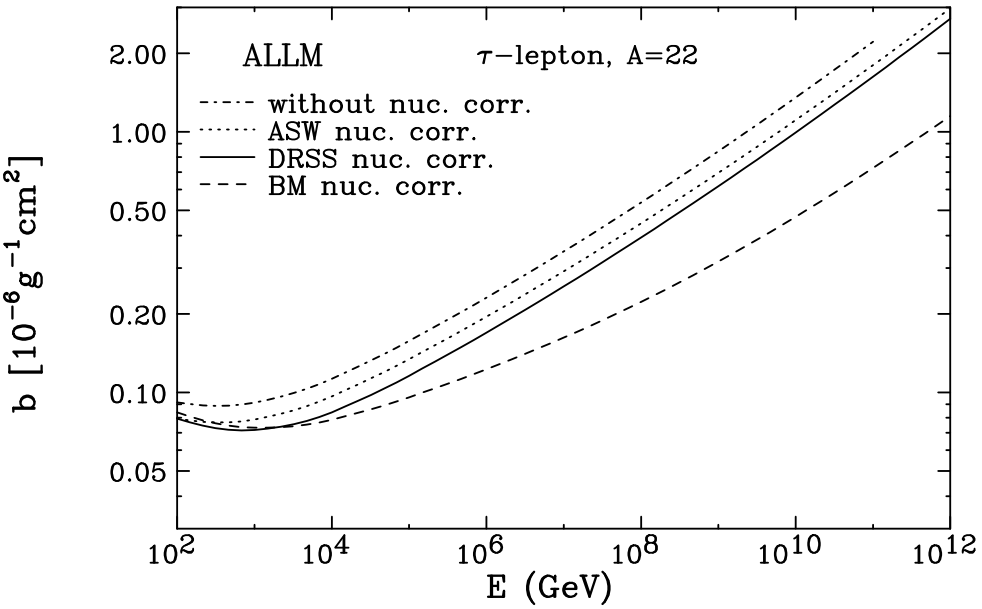

Figure 5: The effect of nuclear corrections on the photonuclear energy loss rate, $b(E)$.

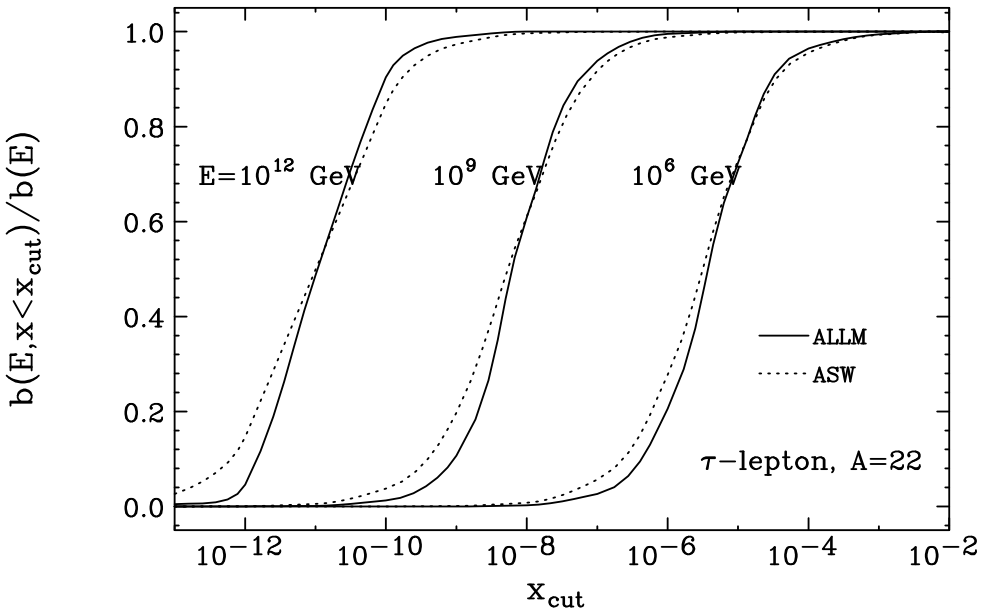

Figure 6: The relative contribution of $x < x_{cut}$ to the photonuclear energy loss rate, $b(E)$.

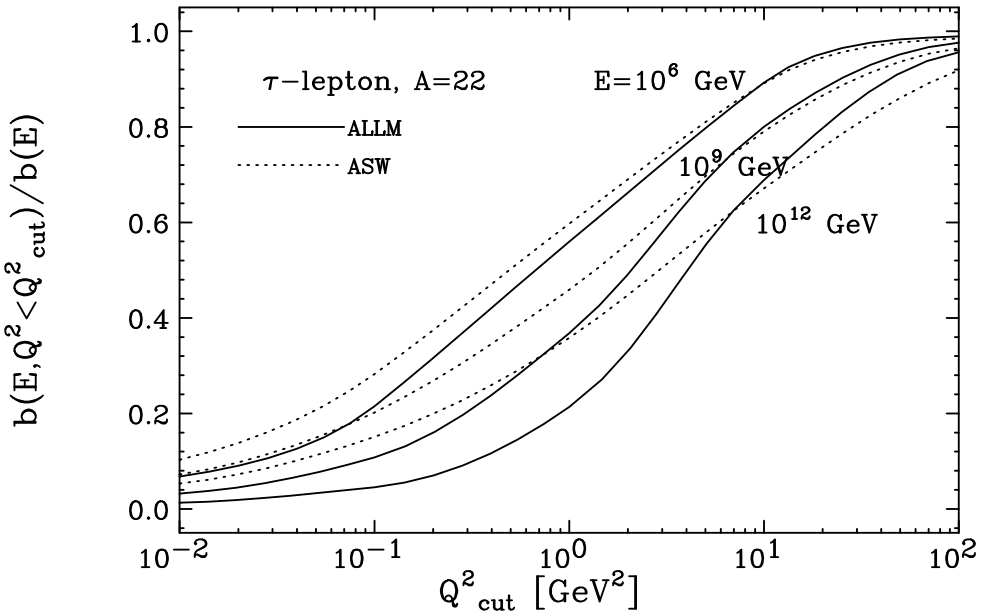

Figure 7: The relative contribution of $Q^2 < Q^2_{cut}$ to the photonuclear energy loss rate, $b(E)$.

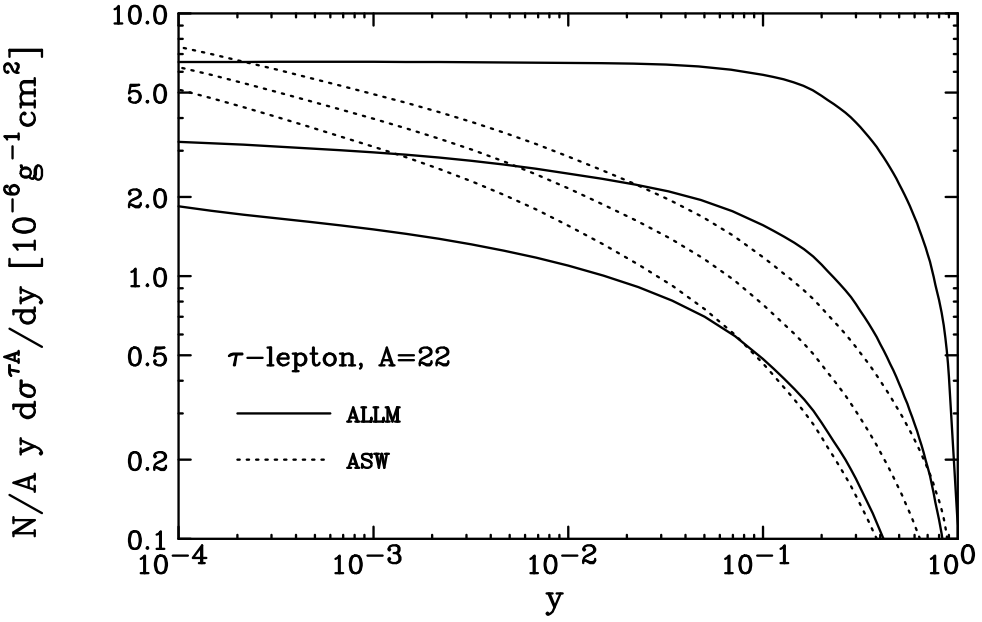

Figure 8: Spectrum of the tau energy loss by photonuclear interactions for tau energies $E = 10^6$, 10^9, and 10^{12} GeV.

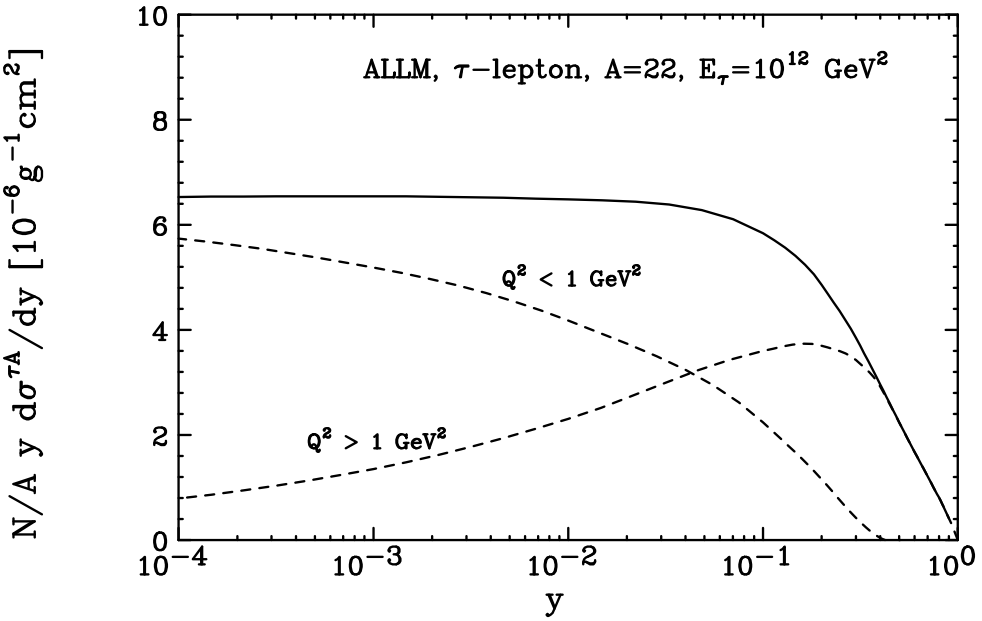

Figure 9: Spectrum of the tau energy loss by photonuclear interactions for a tau of energy $E = 10^{12}$ GeV. The contributions from values above and below $Q^2 = 1$ GeV^2 are shown separately.

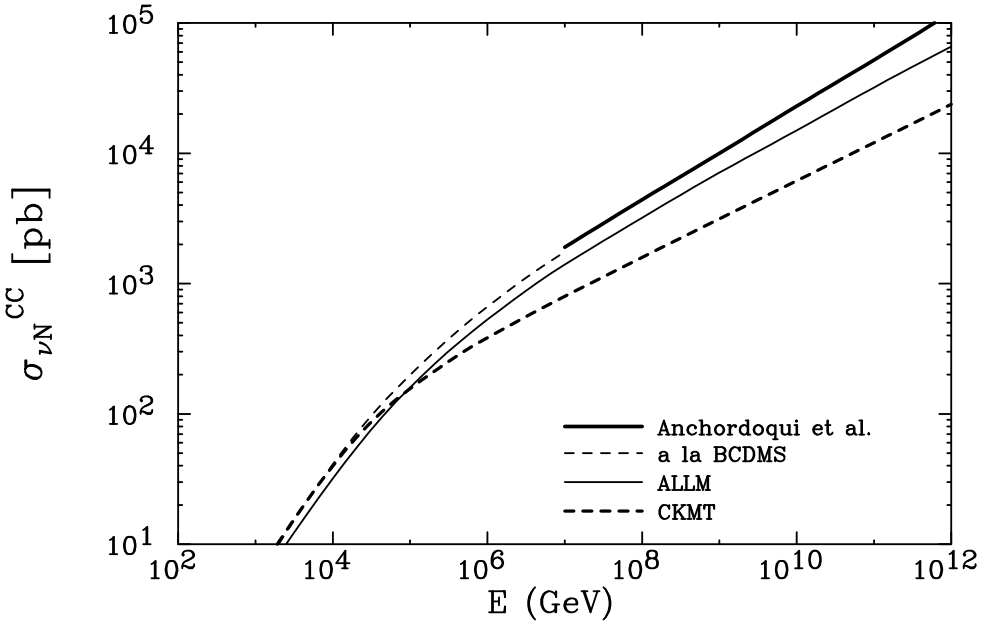

Figure 10: The neutrino-nucleon CC cross section as a function of the neutrino energy, E, from: ALLM, CKMT, SMC *à la* BCDMS structure functions, and the parton density calculation by Anchordoqui *et al.*

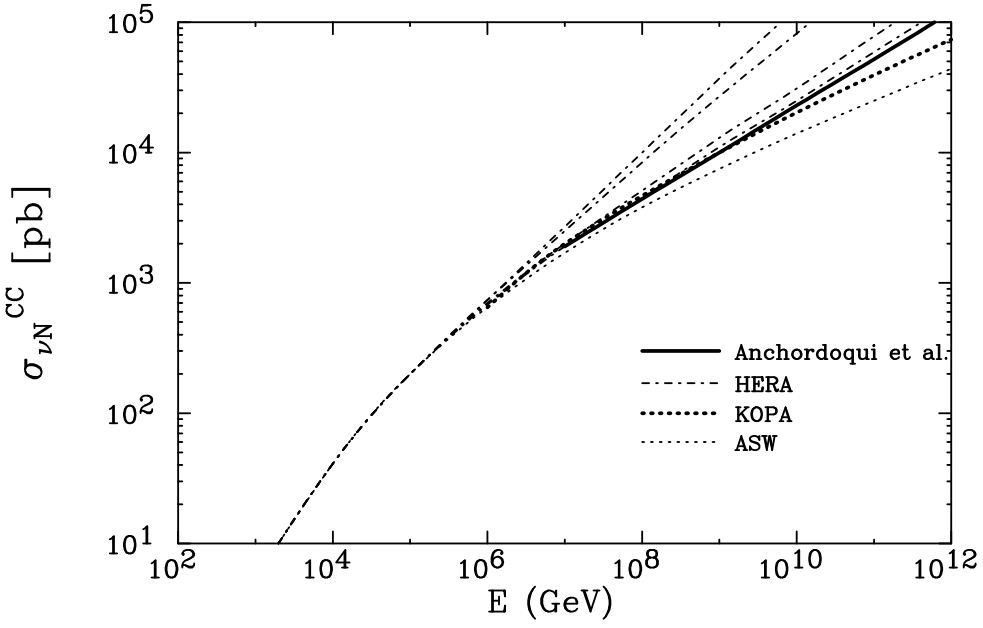

Figure 11: The neutrino-nucleon CC cross section as a function of the neutrino energy, E, from: ASW (extrapolation based on saturation physics), KOPA (extrapolation based on DLA QCD), HERA (phenomenological parameterization of HERA data), and Anchordoqui *et al.* (parton density calculation).